steel research international

Fully Coupled Numerical Analysis of High Frequency Induction Heating and Warm Sheet Metal Forming

Jong Han Park, Jong Bong Kim, and Keun Park*

The present study aims to develop a warm forming process for an aluminum alloy sheet to reduce weight of an electric housing part. Considering that the target product is produced through a series of metal forming processes using a progressive die, high frequency induction heating is proposed to heat a specific drawing punch locally and rapidly, out of a series performed using a progressive die. To validate the effect of the induction heating on the formability improvement of aluminum alloys, a fully coupled numerical simulation is proposed: (i) finite element (FE) analyses for the multi-stage deep drawing processes are performed to predict formability at each stage; (ii) electrostatic-thermal coupled FE analysis is performed to predict the temperature rise of the drawing punch; and (iii) thermo-mechanical coupled analysis is conducted to investigate the effect of induction heating on the formability change. Through the proposed coupled simulation, it is proven that the drawing punch can be efficiently heated without a significant increase in cycle time, and the corresponding drawing process using aluminum alloys can be successfully performed without forming failure.

1.. Introduction

Recent demand to reduce the weight of vehicles and portable electronics parts has driven the use of light metal alloys instead of carbon steels. Among various light metal alloys, aluminum alloys, because of their lightweight, good corrosion resistance, and excellent thermal conductivity, have been popularly used to replace steel parts. However, the low formability of aluminum alloys is a critical drawback when they are used in sheet metal forming.[1] A feasible way to improve the formability of aluminum alloys is the introduction of warm forming in which aluminum sheets are formed under elevated temperature, usually below the recrystallization temperature. Several studies have been performed to investigate the improved forming characteristics of aluminum alloys at elevated temperature.[2–6]

In warm forming, two approaches are available to increase the processing temperature: blank heating or die heating. For the blank heating, the sheet blank is usually preheated to a target temperature, and is then installed on the forming die. This method is advantageous because the die set can be used without any modification while it has drawbacks such as the requirement of blank overheating and relevant blank handling problems. For the heating of a die, on the contrary, a number of heaters are installed in the die set, and the target temperature can be maintained through feedback temperature control. While this method can provide more stable temperature control than the blank heating method, it requires additional modification of the die set for the heater installation.

This study aims to apply warm forming to multi-stage deep drawing processes in which a progressive die is used. A progressive die consists of an array of punches and dies mounted in tandem, and is able to perform various combinations of processes such as blanking, piercing, bending, and drawing.[7] The sheet blank is supplied as a long strip, and each station performs one or more operations sequentially until a finished part is fabricated. Thus, the use of a progressive die causes heating difficulty not only in blank heating but also in punch/die heating. In the case of blank heating, local heating is not possible considering that the sheet parts for each stage are connected to each other and the aluminum alloys have high thermal conductivity. In the case of punch/die heating, conventional heating based on heat conduction increases the die temperature globally because the progressive die set becomes entirely heated even if only a small portion of the die needs to be heated.

In this study, high frequency induction heating is used to raise the surface temperature of a drawing punch locally

[*] J. Park, K. Park
Department of Mechanical System Design Engineering, Seoul National University of Science and Technology, Seoul, Republic of Korea
Email: kpark@seoultech.ac.kr
J. Kim
Department of Mechanical and Automotive Engineering, Seoul National University of Science and Technology, Seoul, Republic of Korea

DOI: 10.1002/srin.201400580

and rapidly. High frequency induction heating uses a high frequency skin effect and electromagnetic induction so that dies or molds can be rapidly heated as an indirect manner.[8,9] The rapid and localized heating capability of induction heating is advantageous in heating a drawing punch out of a progressive die if an induction coil is properly designed to heat the desired region. For this purpose, finite element (FE) analyses for the multi-stage deep drawing processes are performed at first, and the formability of the aluminum alloy is predicted at each stage. An induction coil is designed to reflect the simulation results. Electrostatic-thermal coupled numerical analysis is then performed to predict the temperature change of the drawing punch due to the induction heating. Finally, thermo-mechanical coupled analysis is conducted to investigate the formability change of the aluminum alloy due to high frequency induction heating.

2. Numerical Analysis for Sheet Metal Forming

2.1. Process Overview

This study concerns a multi-stage forming process for an electric housing part in which aluminum sheets must be used to replace the existing steel parts. This multi-stage forming process consists of 16 consecutive processes including four deep drawing processes, all of which are performed using a progressive die. The housing part is a cup shape of which the base diameter and height are 82 mm and 73 mm. Considering that the initial blank diameter is 200 mm, the corresponding drawing ratio is calculated to be 2.44. Because this drawing ratio is too large to be performed in a single drawing process, a multi-stage drawing was used to avoid forming failures. Therefore, the drawing process was divided into four stages, as shown in **Figure 1**, which was applied to the manufacturing of steel parts without any forming failure.

This multi-stage process was industrially used in manufacturing the desired part shape with additional forming processes using a progressive die. Despite the fact that a progressive die is advantageous in its cost efficiency and productivity, it is disadvantageous in the case of warm forming because the conventional heating method based on heat conduction increases the die temperature globally. That is, the entire progressive die set becomes heated even if only a small portion of the die needs to be heated; this leads to a long cycle time for proper die cooling. Therefore, local heating is required to increase the heating efficiency as well as the formability in the failure region.

2.2. Formability Comparison for Various Blank Materials

To compare the formability of steel and aluminum alloys, FE analyses were performed for the four-stage deep

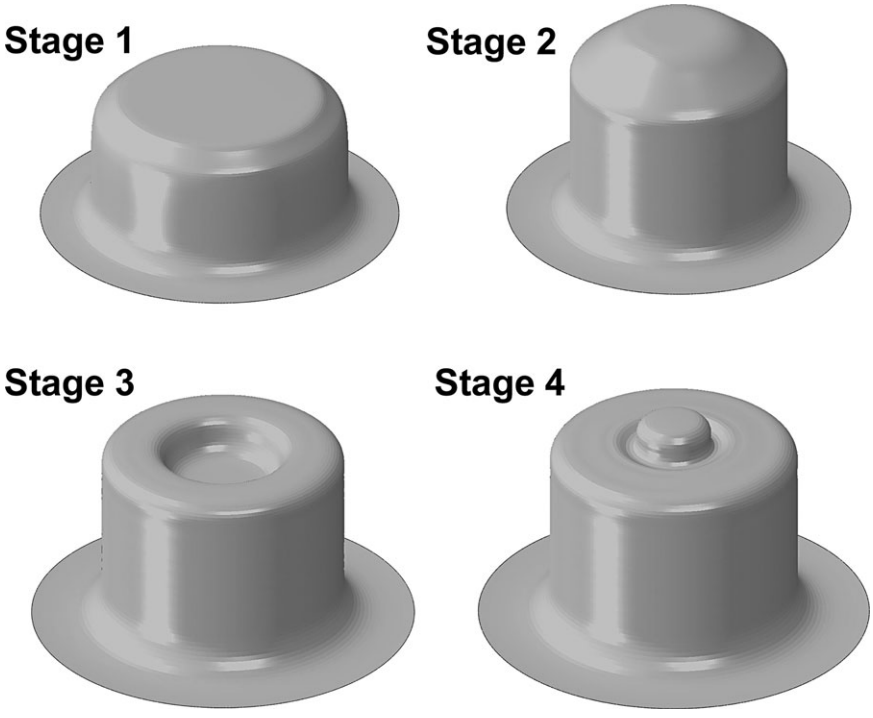

Figure 1. Stepwise description of the multi-stage deep drawing process.

drawing processes. Two blank materials were compared: a cold rolled steel sheet (SPCE) with a thickness of 1.0 mm, and an AA5182-O sheet with a thickness of 1.15 mm. **Table 1** summarizes the mechanical properties required for sheet metal forming simulation.[5,10] ABAQUS Standards® was used for the simulation of the deep drawing processes. Axisymmetric shell elements were used for the simulation, under the elastoplastic constitutive model and the normal anisotropy assumption.

Figure 2a and b shows the estimated thickness distributions after each drawing stage for both materials. Overall, thickness reductions were concentrated on the locally protruded region at the center of the housing where forming failure may occur. In the case of SPCE, the minimum thickness was 0.869 mm after the final drawing stage, which corresponds to 86.9% of the original thickness (1.0 mm). In the case of AA5182-O, on the other hand, the minimum thickness was 0.930 mm, corresponding to 80.9% of the original thickness (1.15 mm). This indicates that the local thinning of AA5182-O is much severe than that of SPCE.

To evaluate the formability of each material quantitatively from the FE analyses, the failure measure based on the forming limit diagram (FLD) was defined as the ratio of the current major principal strain (ϵ_1) to the major limit strain (ϵ_1^*) on the forming limit curve (FLC), as expressed in the following equation:

$$\gamma_{\mathrm{FLD}} = \frac{\epsilon_1(\epsilon_2)}{\epsilon_1^*(\epsilon_2)} \times 100(\%). \quad (1)$$

where, ϵ_1 and ϵ_2 indicate the major and minor principal strain components, respectively. In Equation (1), the major limit statin was determined from FLC by assuming that the strain path is linear. Thus, the failure measure becomes 100% when the given strain state exactly locates on the FLC, and the value higher than 100% indicates that a failure occurs during the forming process. **Figure 3** compares FLCs of SPCE (thickness: 1.0 mm) and AA5182-O (thickness: 1.15 mm) sheets, where FLCs of AA5182-O are plotted for various forming temperatures.[5] Based on these curves, we can determine whether failure occurs or not according to the strain value is located above the FLC at given temperature or not. Thus, the relative location of the major strain value to the corresponding FLC can be changed according to forming conditions such as blank material and forming temperature, which is to be quantified through FE analysis.

Figure 4a and b compares the failure measure distributions at each stage for both materials. In the case of SPCE, the resulting failure measure maintains a value lower than 40% for all stages, as shown in Figure 4a. On the contrary, in the case of AA5182-O, the failure measure exceeds 100% at the fourth stage as shown in Figure 4b. The maximum failure is 120.6% at the fourth stage, which indicates that a forming failure occurs in the outer circumferential region (radial distance: 11.2–17.1 mm), when cold forming was applied. Therefore, this region should be heated properly in order to improve formability by moving FLC at elevated temperature, as illustrated in Figure 3.

3. Coupled Numerical Analysis of Induction Heating and Sheet Metal Forming

3.1. Theoretical Backgrounds

3.1.1. Electromagnetic Field Calculation

In high frequency induction, governing equations to describe electromagnetic fields to given by Equation (1), by introducing the magnetic vector potential **A**.[11]

$$\frac{1}{\mu}\nabla \times \nabla \times A - \sigma\frac{\partial A}{\partial t} = 0 \quad (2)$$

By discretizing Equation (2), FE formulation to predict electromagnetic field is obtained so that the induced eddy current distributions can be calculated; the resulting value will be used in the following heat transfer analysis.

3.1.2. Transient Heat Transfer Analysis

In the high frequency range, it is known that the electric current near the conductor surface is greater than the current in the conductor core, so-called *skin effect*. The skin depth covering 67% of electric current in a conductor is defined by Equation (3):

Blank material	SPCE	AA5182-O
Initial blank thickness (mm)	1.0	1.15
Strength coefficient (MPa)	521.2	539.4
Strain hardening index	0.2323	0.3044
Anisotropy parameter (*R*-value)	1.3165	0.9487

Table 1. Material properties of cold rolled steel (SPCE) and aluminum alloy (AA5182-O)

Figure 2. Thickness distributions after each drawing stage for: (a) SPCE and (b) AA5182-O.

$$\delta = \sqrt{\frac{\sigma}{\pi f \mu_r \mu_0}} \tag{3}$$

where, f is the current frequency, and μ_0 and μ_r are the free space permeability and relative permeability, respectively. Considering that the skin depth decreases as the induced frequency increases, the induced eddy current flows near the mold surface in the case of high frequency induction.[12]

This eddy current is then dissipated as heat, which can be calculated from the estimated current density (J), as expressed in Equation (4). The resulting temperature rise in the mold is calculated by solving Equation (5), the transient heat conduction equation:

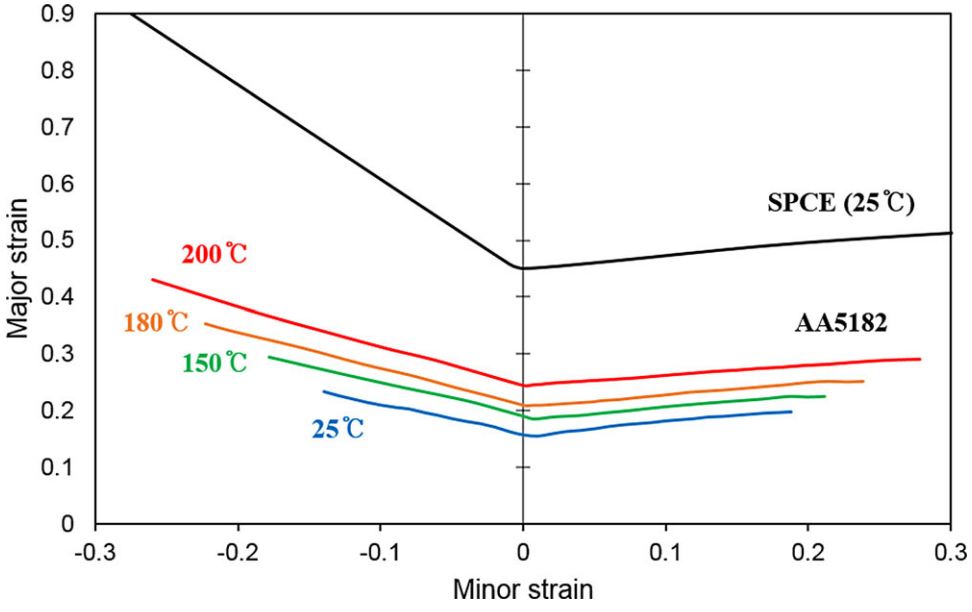

Figure 3. Forming limit curves for SPCE and AA5182-O at various temperatures.[5]

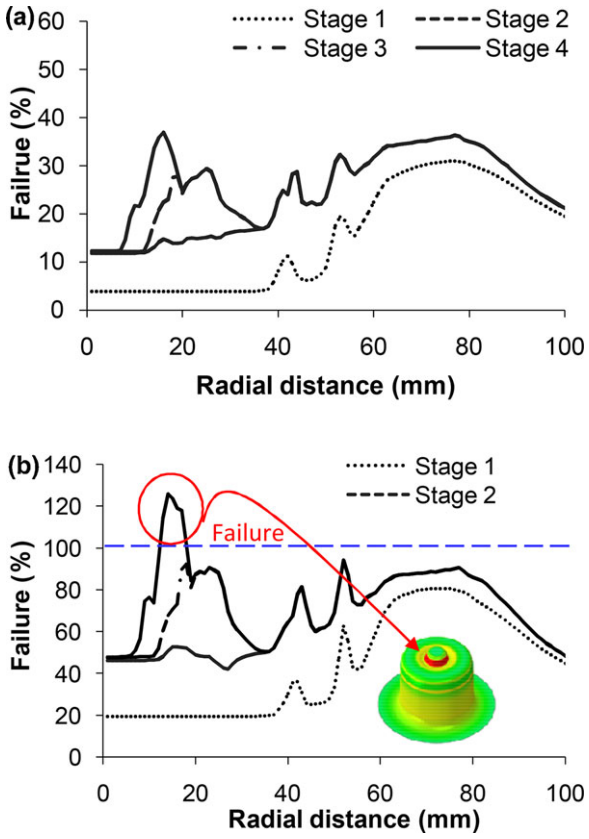

Figure 4. Distributions of the failure measure along the radial distance: a) SPCE and b) AA5182-O sheet.

$$\dot{Q} = \sigma \|\mathbf{J}\|^2 \tag{4}$$

$$\nabla^2[k(T)T] + \dot{Q} = \rho C(T)\frac{\partial T}{\partial t} \tag{5}$$

where, C, k, and ρ are the specific heat, thermal conductivity, and material density, respectively. Considering that some properties of the mold material vary according to its temperature, electromagnetic and thermal analyses should be coupled for the simulation of high frequency induction heating.[13]

3.1.3. Sheet Metal Forming Analysis at Elevated Temperature

For numerical simulation of the sheet metal forming process, a constitutive equation for the sheet material should be defined. A flow rule in which the flow stress is expressed as a function of plastic strain and strain rate is widely used as this constitutive equation, expressed as follows:[14]

$$\bar{\sigma}(\bar{\epsilon}^p, \dot{\epsilon}) = K(\bar{\epsilon}^p + \epsilon_0)^n \left(\frac{\dot{\epsilon}}{\epsilon_{\mathrm{sr0}}}\right)^m \tag{6}$$

where, K, m, and n are the strength coefficient, strain-rate sensitivity index, and strain-hardening exponent. $\dot{\epsilon}$ is the strain rate, $\bar{\epsilon}^p$ is the effective plastic strain, ϵ_0 is the elastic strain constant, and ϵ_{sr0} is the strain rate normalization factor. At elevated temperatures, the material constants (K, m, and n) vary according to the temperature change. Thus, the flow rule in Equation (6) is expressed as follows:

$$\bar{\sigma}(\bar{\epsilon}^p, \dot{\epsilon}, T) = K(T)(\bar{\epsilon}^p + \epsilon_0)^{n(T)} \left(\frac{\dot{\epsilon}}{\epsilon_{sr0}}\right)^{m(T)}. \tag{7}$$

Through the induction heating simulation, the temperature fields of the heated punch are obtained. The local temperature rise in the sheet metal can then be predicted through the heat transfer analysis, from which the temperature-dependent flow rule can be applied during the sheet metal forming process.

3.2. Electrostatic-Thermal Coupled Analysis for Punch Heating Simulation

To investigate the effect of high frequency induction on mold surface heating, an electrostatic-thermal coupled FE analysis was performed. Based on the results shown in Figure 4(b), induction heating was applied to the drawing punch of the fourth stage. Considering that the failure region (between 11.2 mm and 17.1 mm in radial distance in Fig. 4b) is limited in the local region where a small cup shape is formed, heating is required in this region for formability improvement.

Figure 5a provides a configuration of the heating section, consisting of a drawing punch and an induction coil. The coil is 5 mm in diameter; it is located at a distance of 2 mm from the punch. The punch material is H20 steel, of which the relative permeability is 400. As boundary conditions, a coil current of 300 A and 160 kHz was applied for 5 s. Coupled FE analysis was performed by connecting the electromagnetic and thermal analyses, using ABAQUS Standards®.

Figure 5b shows magnetic flux lines in the analysis domain, which indicates that the magnetic fields are concentrated on the outer region of the punch tip. Thus, the induction heating effect is expected to be concentrated on that region. Figure 5c shows the resulting temperature distribution at the end of induction heating. A maximum temperature of 528.7 °C was obtained on the outer surface, while the temperature of the remaining region was still lower than 300 °C. This result indicates that the drawing punch can be locally heated in a short time, with the heating mainly concentrated near the failure region. To compare the heating characteristics of the punch surface, temperature variations at three sample points (P_1, P_2, and P_3) are plotted in Figure 5d. It can be seen that the punch temperatures increase during the heating period and then

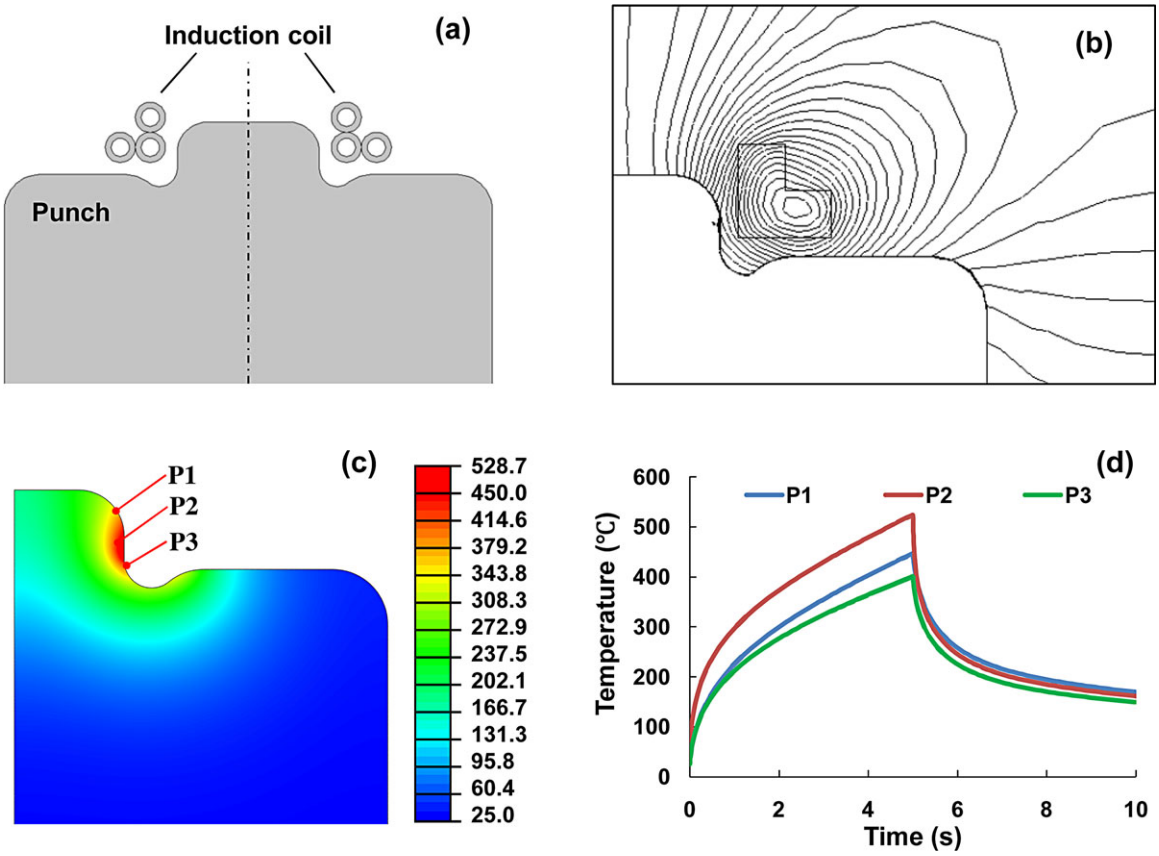

Figure 5. FE analysis results for high-frequency induction heating: (a) analysis domain, (b) magnetic flux lines, (c) temperature distribution after 5 s heating, and (d) temperature change at various locations.

decrease rapidly after heating, which means that it is possible to obtain rapid heating and cooling in a short period of heating time. Furthermore, temperatures in the failure region (P_1 and P_2) are still maintained higher than 200 °C even after the 5 s of cooling, which is sufficient for the proposed process to be regarded as warm forming in that region.

3.3. Thermo-Mechanical Coupled Analysis for Sheet Metal Forming Simulation

To investigate the effect of the localized induction on the formability change, sheet metal forming simulation was conducted for the fourth drawing process by imposing the induction heating simulation results as thermal boundary conditions. The material constants (*K*, *n*, *m*, and *R*-value) of AA5182-O in the high temperature range were taken from the previous research.[5] The thermal boundary condition was interactively calculated and applied to consider the heat transfer effect in the locally heated region;[12] this heat transfer effect includes heat transfer among the heated punch, AA5182-O sheet, and drawing die. To describe the temperature change in the AA5182-O sheet, the sheet blank was numerically modeled using four-node rectangular continuum elements.

Figure 6 a shows the temperature changes during the drawing process. It can be seen that the highest temperature region was the outer circumferential surface of the punch at the beginning of the drawing process (T_{max}: 532.4 °C). The highest temperature region then moved to the center region as the drawing process continued. This can be explained by heat conduction from the heated punch to the contacted sheet metal, from which the flat face of the protruded part showed a higher temperature than that of the outer circumferential region. Figure 6 b provides an enlarged view of the temperature distribution after the final stage, in which the contour bar was rearranged according to the temperature range at this stage (T_{max}: 223.6 °C). It can be seen that the temperature of the flat face of the protruded sheet is higher than 200 °C while that of the outer failure region is less than 150 °C. This indicates that the formability of the flat region is better than that of the outer region. Therefore, a local thinning region is expected to be moved from the outer region to the flat region due to local stretching deformation mode.

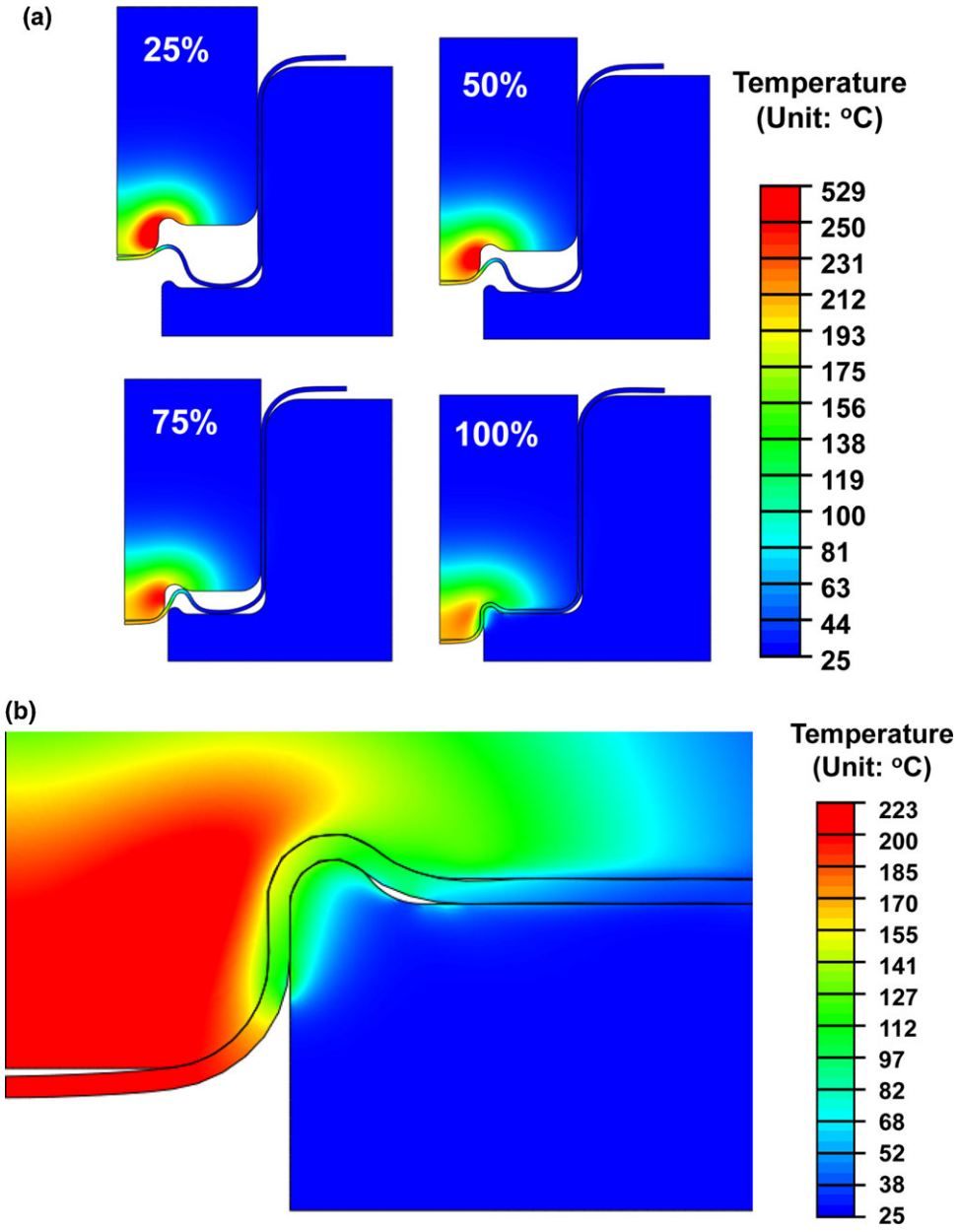

Figure 6. Thermo-mechanical analysis results for the warm forming of AA5182-O: (a) temperature changes during the deep drawing process and (b) an enlarged view for the failure region at 100% stroke.

4. Results and Discussion

To compare formability of the proposed warm forming with the conventional cold forming, the failure measure and thickness distribution are compared in **Figure 7**. In these graphs, the radial distance is limited to 30 mm in which area the local thinning and failure are concentrated. Figure 7a compares the failure distributions of warm forming with that of cold forming. It can be seen that the failure measure does not exceed 100% in the case of warm forming due to the formability improvement at elevated temperatures, as described in Figure 3. The maximum failure measure was 99.4%, which corresponds to 82.4% of the cold forming result.

Figure 7b compares the thickness distributions in both cases. It is notable that the thickness in warm forming is greater than that in cold forming in the failure region (between 11.2 mm and 17.1 mm in radial distance). In contrast, warm forming leads to a smaller thickness in the flat region, of which the radial distance is less than 8.0 mm. This can be explained by the temperature distribution shown in Figure 6b, in which the flat region shows a higher temperature than that of the outer failure region. Therefore, the local thinning in the failure region can be

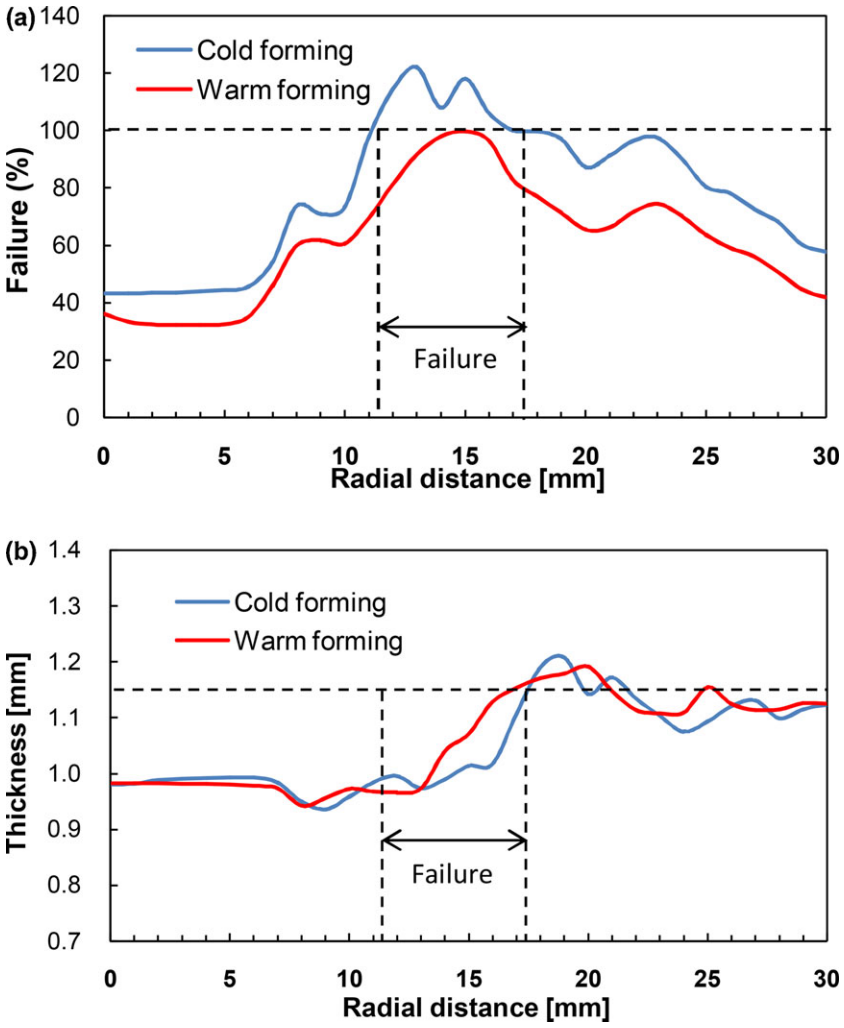

Figure 7. Comparison of the cold and warm forming for the warm forming of AA5182-O after the 4th drawing stage: (a) failure measure and (b) thickness distribution.

alleviated, which additionally improves the formability during the localized warm forming.

5. Conclusion

In this study, a multi-stage deep drawing process was developed to change the blank material from a cold rolled steel (SPCE) sheet to an aluminum alloy (AA5182-O) sheet. FE analyses were performed to predict the formability in both cases, and a failure was detected at the fourth stage in the case of AA5182-O. To improve the formability of the corresponding process, warm forming was developed by the use of high frequency induction heating. Owing to the rapid and localized heating capability of high frequency induction heating, it was possible to easily and efficiently heat a drawing punch out of a series of a progressive dies without a global die heating. To investigate the effect of high frequency induction heating on the formability improvement of an AA5182-O sheet, fully coupled FE analyses were used by connecting electromagnetic field calculation, transient heat transfer analysis, and sheet metal forming simulation. Through the simulation results, it was found that the failure measure could be reduced by 18% by the virtue of locally elevated temperature. Although the maximum failure measure of 99.4% may not be acceptable for implementation in industrial forming processes, the proposed coupled simulation provided guidelines for further formability improvement by suggesting enhanced heating conditions or thicker sheet blank, from which an appropriate design for the industrial warm forming process could be realized.

Acknowledgement

This research was financially supported by Basic Science Research Program through the National Research Foundation (NRF) funded by the Ministry of Education, Republic of Korea, Grant No. NRF-2013R1A1A2A10004709.

Received: December 10, 2014;
Published online: February 5, 2015

Keywords: aluminum alloys; warm forming; progressive die; high frequency induction heating; finite element analysis

References

[1] S. Toros, F. Ozturk, I. Kacar, *J. Mater. Process. Technol.* **2008**, *207*, 1.
[2] A. H. Van den Boogaard, J. Huétink, *Comp. Meth. Appl. Mech. Engng.* **2006**, *195*, 6691.
[3] N. Abedrabbo, F. Pourboghrat, J. Carsley, *Int. J. Plast.* **2006**, *22*, 314.
[4] N. Abedrabbo, F. Pourboghrat, J. Carsley, *Int. J. Plast.* **2006**, *22*, 342.
[5] N. Abedrabbo, F. Pourboghrat, J. Carsley, *Int. J. Plast.* **2007**, *23*, 841.
[6] J. Li, J. E. Carsley, T. B. Stoughton, L. G. Hector, Jr, S. J. Hu, *Int. J. Plast.* **2013**, *45*, 21.
[7] K. Park, S. R. Choi, *J. Mater. Process. Technol.* **2002**, *130*, 477.
[8] D. Yao, S. C. Chen, B. H. Kim, *Adv. Polym. Technol.* **2008**, *27*, 233.
[9] K. Park, D. H. Sohn, K. H. Cho, *J. Mech. Sci. Technol.* **2010**, *24*, 149.
[10] S. Panich, V. Uthaisangsuk, J. Juntaratin, S. Suranuntchai, *J. Metals Mater Miner.* **2011**, *21*, 19.
[11] K. R. Demarest, *Eng. Electromagn.* Prentice Hall, New-Jersey **1998**.
[12] H. Eom, K. Park, *Polym. Plast. Technol. Engng.* **2009**, *48*, 1070.
[13] H. Eom, K. Park, *Int. J. Precis. Eng. Manuf.* **2011**, *12*, 53.
[14] R. H. Wagoner, J-L. Chenot, *In Fundamentals of Metal Forming*, Wiley, New York **1996**.